A Compact Circularly Polarized Slotted Patch Antenna for GNSS Applications

Nasimuddin, Xianming Qing, and Zhi Ning Chen

Abstract —**A compact circularly polarized (CP) square-ring slotted patch antenna with vias is proposed for global navigation satellite systems (GNSS). Four square-ring-shaped slots are cut symmetrically onto a square patch radiator along its diagonals for wide-angle CP radiation and miniaturization. The antenna size is further reduced by grounding the central patches surrounded by the square-ring-shaped slots. An antenna prototype with an overall size of 60 mm × 60 mm × 5 mm shows a measured 10-dB return loss bandwidth of 90.0 MHz (1.565–1.655 GHz) with a maximum gain of 4.65 dBic. The measured 3-dB axial ratio (AR) bandwidth is 35.0 MHz (1.57–1.605 GHz) with a 3-dB AR beamwidth of more than 140° across the bandwidth.**

Index Terms — Circularly polarized antenna, GNSS, patch antenna, miniaturization, slotted patch radiator, via.

I. Introduction

Global navigation satellite systems have been used in many areas such as navigation, positioning, public safety and surveillance, geographic surveys, time standards, mapping, weather, and atmospheric information. The overall size of this kind of system is getting smaller and the signal strength being received is always weak, thus, a compact circularly polarized (CP) antenna with medium gain (about 5 dBic) is highly demanded, in particular, for portable terminals. CP antennas are able to offer a reliable system connection because polarization of the antennas is always aligned. Furthermore, the CP antenna with one CP sense (for example, right-hand circular polarization, RHCP) carries the characteristic that is able to reject the signal of the opposite CP sense (for example, left-hand circular polarization, LHCP), which is effective for multi-path interferences suppression [1-3]. In general, a compact GNSS antenna is required to be with RHCP radiation, medium gain and wide AR beamwidth, wherein the size and AR beamwidth are more critical compared with the gain and bandwidth of the antenna. Generally, an antenna covering one of the GNSS bands with a bandwidth of few MHz and gain of 4-5 dBic is acceptable [3, 4].

A single-feed CP patch antenna is compact as compared with a dual-feed CP patch antenna at a price of limited gain, narrow bandwidths of AR and impedance. A number of single-feed CP patch antennas have been reported, wherein different radiators such as slit-patch, slotted-patch radiators have been utilized to generate CP radiation [5-10]. Recently, miniaturizations of the CP patch antennas have been proposed using patches based on reactive impedance surface (RIS), mushroom, and complementary split-ring resonators (CSRRs) [11-15]. A compact CP patch antenna loaded with metamaterials was proposed in [11]. The RIS and mushroom-like CRLH structures have been used to miniaturize the CP patch antenna ($0.293\lambda_o \times 0.293\lambda_o \times 0.026\lambda_o$ at 2.58 GHz). The antenna was designed on a low-loss thick dielectric substrate with a gain of 2.98 dBic. In [12], the miniaturization of the CP patch antenna has been achieved using RIS with CSRRs. The antenna has a measured gain of 3.7 dBic and 3-dB AR bandwidth of 1.1%. A single-feed metamaterial-based CP patch antenna with compact size ($0.435\lambda_o \times 0.435\lambda_o \times 0.02\lambda_o$ at 3 GHz) was proposed in [13] with a 3-dB AR bandwidth of 1.05%.

Some techniques have been reported to widen the AR beamwidth of the CP patch antennas, such as using the material with high permittivity, small ground plane size, and multilayer configuration. Recently, a compact double-layer structure, comprising a circular patch with two stubs and a parasitic ring, was proposed in [15]. The overall size of the antenna is $0.57\lambda_o \times 0.57\lambda_o \times 0.11\lambda_o$ at 2.5 GHz with a 3-dB AR beamwidth of 140°.

In this paper, a compact square-ring slotted patch antenna is investigated for GNSS applications. The slotted patch antenna with vias features a compact size and wide-angle CP radiation. The slight difference of the slots on the patch enables the radiator to generate two orthogonal modes with a 90° phase difference and therefore, causes a CP radiation. The square-ring-shaped slots as well as the grounded vias contribute to the antenna miniaturization. The proposed antenna is simulated using the CST Microwave Studio [16] and validated by measurement.

II. Antenna Design

The cross-sectional view of the proposed square-ring slotted patch antenna with vias is shown in Fig. 1(a), wherein the patch lies in the *x-y* plane and the center of the square patch radiator aligns with the origin of the Cartesian coordinate system. The length of the square slotted patch radiator and ground plane is denoted by L and G_p, respectively. The feed is positioned along the –*x*-axis with a distance of x_o from the center of the patch. The centers of four square-ring-shaped slots are located along the diagonal line directions at points [($\pm s$, $\pm s$), where $s = L/4$] of the patch radiator as shown in Fig. 1(b). The square-ring-shaped slots are with length and width of (s_1, g_1) and (s_2, g_2), respectively. The inner patches surrounded by the square-ring-shaped slots are centrally grounded through vias with a radius of V_r.

By slightly changing the length or width of one slot pair, the proposed antenna is able to generate CP radiation. The antenna is RHCP with a coaxial feed located along the *x*-axis and LHCP along the *y*-axis. The sense of CP radiation can also be altered by exchanging the pair of smaller or bigger square-ring-shaped slots. The dimensions of the optimized antenna at the operating frequency of 1.6 GHz for RHCP radiation with wide beamwidth and compact size are L=40.9 mm, s_1 = 8.65 mm, s_2 = 6.35 mm, g_1 = g_2 = 0.5 mm, $s'_1 = s_1 –$

Authors are with the Institute for Infocomm Research, A*STAR, 1 Fusionopolis Way, #21-01 Connexis (South Tower), Singapore 138632. (e-mail: nasimuddin@i2r.a-star.edu.sg, qingxm@i2r.a-star.edu.sg, chenzn@i2r.a-star.edu.sg).

Zhi Ning Chen is also with Department of Electrical and Computer Engineering, National University of Singapore (eleczn@nus.edu.sg).

$2g_1$ = 7.65 mm, $s'_2 = s_2 - 2g_2$ = 5.35 mm, x_o = 8.5 mm, H = 5.0 mm, substrate dielectric constant, ε_r = 3.4, loss tangent = 0.0027, coaxial feed diameter, f_d = 1.27 mm, and V_r = 0.75 mm. The optimized antenna design will be used as the reference for the parametric studies in the succeeding sections.

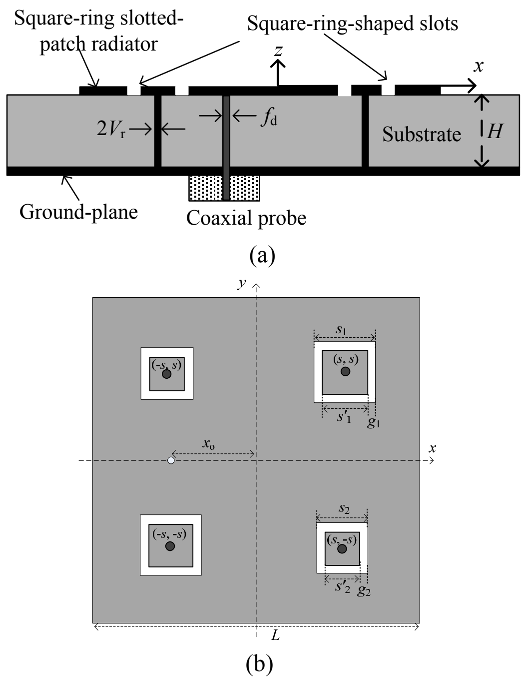

Fig. 1. Proposed antenna geometry: (a) cross-sectional view and (b) top view.

A. Comparison of the CP patch antennas

Fig. 2 compares the performance of the proposed antenna and a truncated CP patch antenna in terms of return loss, AR, and gain, where the size of the ground plane (60 mm × 60 mm), the patch radiator (40.9 mm × 40.9 mm), substrate thickness of 5.0 mm, and diameter of the coaxial feed probe of 1.27 mm are kept unchanged. Both antennas exhibit the desired impedance matching, AR bandwidth, and gain. However, the operating frequency of the proposed antenna is 1.58 GHz much lower than 1.838 GHz of the truncated patch antenna. The operating frequency of the proposed antenna without vias is 1.805 GHz. It implies that the proposed antenna realizes a 20% size reduction compared with the truncated patch antenna if both antennas operate at the same frequency. The size reduction of the proposed antenna attributes to the longer current path on the radiator and the additional capacitive loading from the square-ring-shaped slots as well as the inductive loading from the vias.

B. Operating mechanism and current density distributions

The two orthogonal modes with a 90° phase difference for CP radiation are excited by introducing asymmetries to the square patch radiator, wherein the size of the square-ring-shaped slot pair along the 135° diagonal line direction is a bit smaller than the one along the 45° diagonal-line direction. The current density distributions of the proposed antenna in xy-plane at z = 0 as ωt = 0°, 45°, 90°, and 135° are illustrated in Fig. 3. The time-dependent rotating current density distributions are clearly observed, which validate the CP radiation from the proposed antenna.

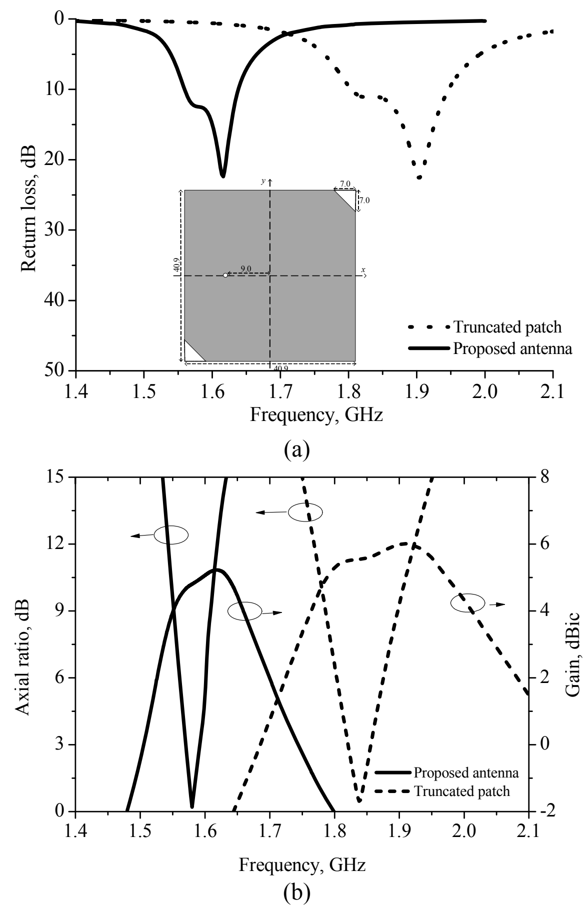

Fig. 2. Comparison of the CP patch antennas: (a) return loss; (b) AR and gain at the boresight.

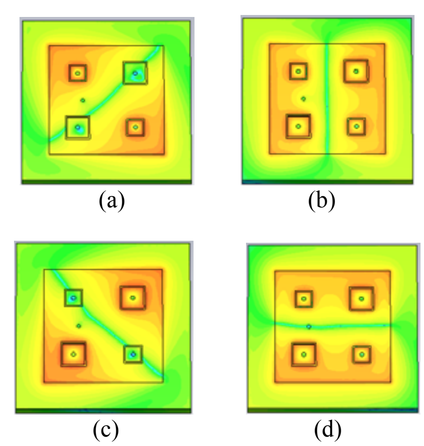

Fig. 3. Current density distributions of the proposed antenna at 1.58 GHz.

III. Parametric Studies

Parametric studies are conducted by simulation to examine the effects of the antenna parameters on the AR performance of the proposed antenna, and to provide engineers with more information regarding the antenna design and optimization. Unless specially indicated, only one geometrical parameter is varied each time and the rest are kept unchanged.

A. *Length of the inner patch of the bigger square-ring-shaped slot, s'_1*

The AR at the boresight is shown in Fig. 4 when the length (s'_1) of the inner patch of the bigger square-ring-shaped slot varies from 6.55 to 8.15 mm. As s_1 is fixed, the width of the slot, g_1, is changed as $g_1 = (s_1\text{-}s'_1)/2$. Increasing s'_1, causes the operating frequency to shift down while the AR exhibits an interesting response: the desired AR is observed first for a smaller s'_1 = 6.55 mm; it degrades for s'_1 = 7.35 mm and becomes optimal when s'_1 = 7.65 mm; and for s'_1 = 8.15 mm, the AR is larger than 13 dB, which indicates that the radiation at the operating frequency is linearly polarized. Because CP radiation is caused by the slight difference between the square-ring-shaped slot pairs, the two orthogonal resonant modes will not be maintained once the difference between the slot pairs exceeds to some extent.

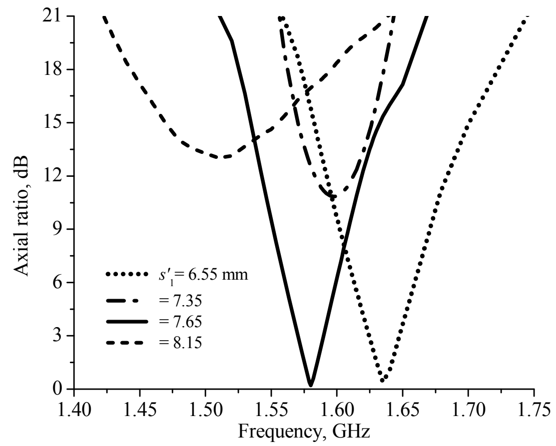

Fig. 4. Axial ratio with varying inner patch lengths of the bigger square-ring-shaped slot, s'_1.

B. Length of bigger square-ring-shaped slot, s_1

The AR with varying lengths of the bigger square-ring-shaped slot, s_1, is exhibited in Fig. 5. The response of AR against frequency is similar to varying s'_1. When s_1 increases from 8.15 to 10.15 mm, the operating frequency shifts down while the AR shows a big variation.

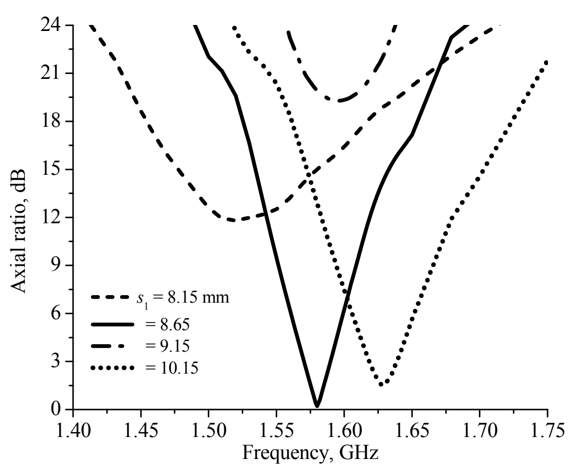

Fig. 5. Axial ratio with varying lengths of the bigger square-ring-shaped slot, s_1.

C. *Length of the inner patch of the smaller square-ring-shaped slot, s'_2*

The length of the inner patch of the smaller square-ring-shaped slot, s'_2, varies from 3.85 to 5.85 mm. With the fixed s_2, the width of the smaller slot, $g_2 = (s_2\text{-}s'_2)/2$, is changed. As shown in Fig. 6, the larger s'_2 lowers the operating frequency with better AR response. When s'_2 is smaller, such as 3.85 mm, the two orthogonal resonant modes are separated far away so that the CP radiation cannot be achieved.

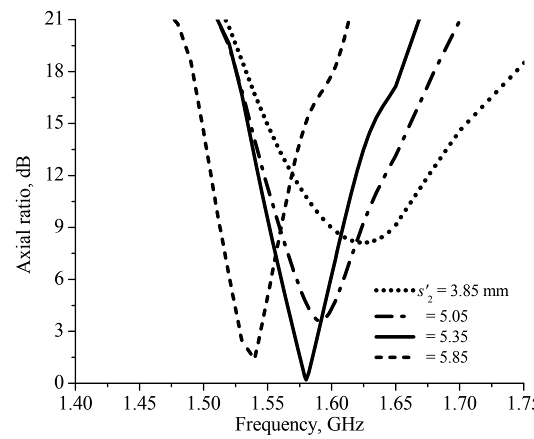

Fig. 6. Axial ratio with varying inner patch lengths of the smaller square-ring-shaped slot, s'_2.

D. Length of smaller square-ring-shaped slot, s_2

The effect of the length of smaller square-ring-shaped slot, s_2, on AR at the boresight is exhibited in Fig. 7, wherein s_2 varies from 5.85 to 7.85 mm. As s'_2 is fixed, the width of the slot, g_2 is changed. Similar to varying s'_2, the operating frequency decreases with increasing s_2. An optimal AR can be achieved with a specific s_2.

E. Via radius, V_r

The effect of the varying radius of via, V_r on the AR performance is shown in Fig. 8 with V_r changing from 0.25 to 1.25 mm. The operating frequency decreases with increasing V_r. The minimum AR at 1.58 GHz is achieved for a radius of 0.75 mm and AR is degraded when V_r diverges from 0.75 mm.

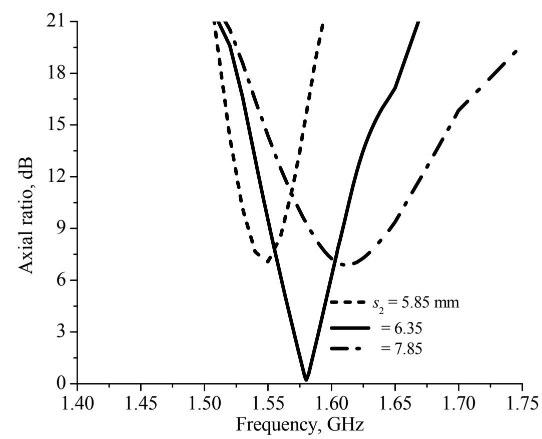

Fig. 7. Axial ratio with varying lengths of the smaller square-ring-shaped slot, s_2.

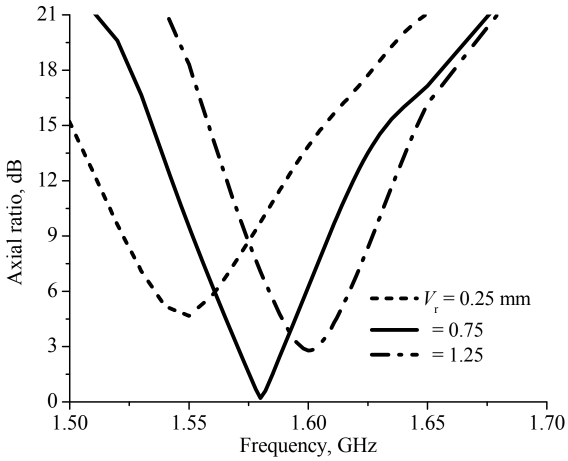

Fig. 8. Axial ratio with varying radii of via, V_r.

F. *Ground plane size (G_p×G_p) and substrate thickness (H)*

Impedance matching improves and the antenna gain increases with larger ground-plane size. The operating frequency decreases with increasing substrate thickness, *H*. For brevity, the performance is not discussed in details.

IV. Experimental Results and Discussions

The proposed antenna was fabricated and tested. The photo of the prototype antenna is shown in Fig. 9(a). The measured and simulated return loss, as well as the AR and gain at the boresight are plotted in Fig. 9. The measured 10-dB return loss bandwidth is 90 MHz (1.57−1.66 GHz). The measured 3-dB AR bandwidth is 35 MHz (1.57−1.61 GHz), which is able to cover GPS L1 band at the center frequency of 1575.42 MHz with a bandwidth of 20.46 MHz [3]. The measured maximum boresight gain is 4.65 dBic at 1.62 GHz. The gain is more than 4.0 dBic over the 3-dB AR bandwidth. The measured results agree with the simulated ones very well.

The radiation patterns of the antenna prototype were measured with a rotating transmitting horn antenna method. Figs. 10(a) and (b) show the measured and simulated normalized radiation patterns in *xz*- and *yz*-planes, respectively, at 1.578 GHz. The 3-dB AR beamwidth is more than 140° in both planes.

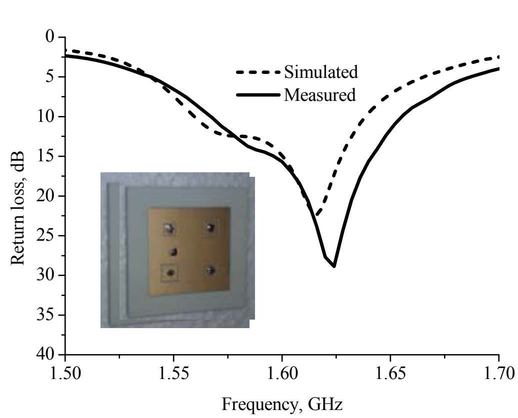

(a)

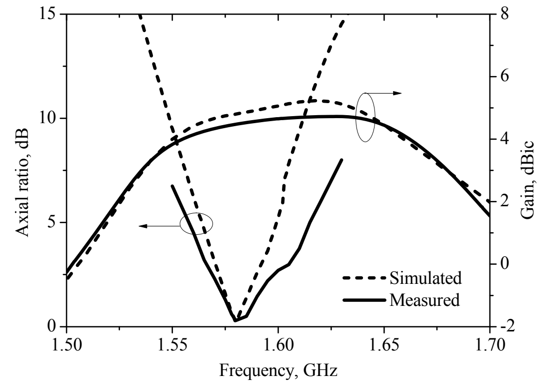

(b)

Fig. 9. Simulated and measured results: (a) return loss and (b) AR and gain at the boresight.

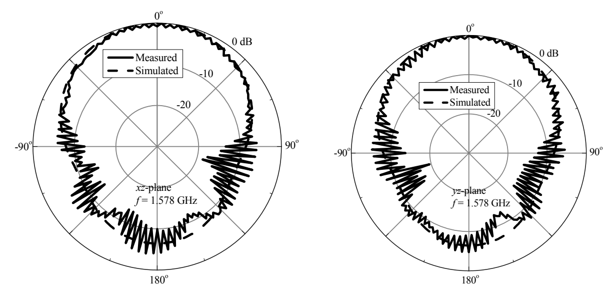

(a) (b)

Fig. 10. Measured and simulated radiation patterns at 1.578 GHz: (a) *xz*-plane and (b) *yz*-plane.

V. Conclusion

A compact square-ring slotted patch antenna with vias has been explored for GNSS applications. Parametric studies have been conducted to understand the CP generation and antenna miniaturization mechanism. It has been found that the performances of the proposed antenna are sensitive to the width/length of the square-ring-shaped slot and the via diameter. The proposed antenna has achieved compact size, medium gain, and wide beamwidth, promising for GNSS applications.

References

[1] B. R. Rao, W. Kunysz, R. Fante and K. McDonald, 'GPS/GNSS Antennas,' Artech House 2013.

[2] Global Positioning Systems Wing (GPSW), Systems Engineering & Integration, Interface Specification: IS-GPS-200 rev D, Mar 2006, available at www.losangeles.af.mil/shared/media/document/AFD-070803-059.pdf.

[3] J. H. Wang, "Antennas for global navigation satellite system (GNSS)," *Proceeding of the IEEE*, vol. 100, no. 7, pp. 2349–2355, July 2012.

[4] G. Z. Rafi, M. Mohajer, A. Malarky, P. Mousavi and S. Safavi-Naeini, "Low-profile integrated patch antenna for GPS-DSRC application," *IEEE Antennas and Wireless Propagation Letters*, vol. 8, pp. 44–48, 2009.

[5] K. L Wong and Y. F Lin, "Circularly polarized patch antenna with a tuning stub," *Electronics Letters,* vol. 34, no. 9, pp 831–832, 1998.

[6] H. M. Chen and K. L. Wong, "On the circular polarization operation of annular-ring patch antennas," *IEEE Trans. Antennas and Propagation*, vol. 47, pp. 1289–1292, 1999.

[7] W. S. Chen, C. K. Wu and K. L. Wong, "Novel compact circularly polarized square patch antenna," *IEEE Trans. Antennas and Propagation*, vol. 49, pp. 340–342, 2001.

[8] J. S. Row and C. Y. Ai, "Compact design of single-feed circularly polarized patch antenna," *Electronics Letters*, vol. 40, no. 18, pp. 1093–1094, 2004.

[9] Nasimuddin, X. Qing and Z. N. Chen, "A compact circularly polarized cross-shaped slotted patch antenna," *IEEE Trans. Antennas Propagation*, vol. 60, no. 3, pp. 1584−1588, March. 2012.

[10] Nasimuddin, X. Qing and Z. N. Chen, "Asymmetric-circular shaped slotted patch antennas for circular polarization and RFID applications," *IEEE Trans. Antennas Propagation,* vol. 58, no. 12, pp. 3821–3828, Dec. 2010.

[11] Y. Dong, H. Toyao and T. Itoh, "Compact circularly-polarized patch antenna loaded with metamaterials," *IEEE Trans. Antennas Propagation*, vol.59, no. 11, pp. 4329−4333*,* Nov. 2011.

[12] Y. Dong, H. Toyao and T. Itoh, "Design and characterization of miniaturized patch antennas loaded with complementary split-ring resonators," *IEEE Trans. Antennas Propagation*, vol. 60, no. 2, pp. 772−785, Feb. 2012.

[13] H. X. Xu, G. M. Wang, J. G. Liang, M. Q. Qi and X. Gao, "Compact circularly polarized antennas combining meta-surfaces and strong space-filling meta-resonators," *IEEE Trans. Antennas and Propagation*, vol. 61, no. 7, pp. 3442−3450, July 2013.

[14] K. Agarwal, Nasimuddin and A. Alphones, "RIS based compact circularly polarized patch antennas," *IEEE Trans. Antennas and Propagation*, vol. 61, no. 2, pp. 547–554, Feb. 2013.

[15] Z. K. Pan, W. X. Lin and Q. X. Chu, "Compact wide-beam circularly-polarized patch antenna with a parasitic ring for CNSS application," *IEEE Trans. Antennas and Propagation*, vol. 62, no. 5, pp. 2847−2850, 2014.

[16] CST Microwave Studio, Version 2013.06, Jan 15 2014.